

Chapter 4

**Equatorial Arabian Sea: SW Monsoon,
NE Monsoon and Intermonsoon
Variations during the Past 35,000 years**

4.1. Introduction:

The equatorial/southern Arabian Sea is the least studied region of the Arabian Sea as most of the studies have focused on either the western/northern Arabian Sea (Prell et al, 1980; Prell and Kutzbach, 1987; Clemens et al, 1991; Anderson and Prell, 1993; Sirocko et al, 1993; Naidu et al, 1993; Naidu and Malmgren, 1995; Reichart et al, 1997, 1998, 2004; Schulz et al, 1998; Gupta et al, 2003; Von Rad et al, 1999; Burns et al, 1998; Neff et al, 2001; Fleitmann et al, 2003; Schulz et al, 1998) or the eastern Arabian Sea (Agnihotri et al, 2003a, 2003b; Sarkar et al, 2000; Thamban et al, 2001). Nevertheless, the equatorial Arabian Sea is very important to paleoclimatic studies as it experiences the effect of Southwest monsoon as well as Northeast monsoon (Duplessy, 1982; Sarkar et al, 1990) unlike the above-mentioned other two regions, which are affected mostly by the SW monsoon. It has been proposed that during LGM, the SW monsoon was weaker (Prell et al, 1980; Van Campo et al, 1982) with a feeble indication of stronger NE monsoon than at present (Duplessy, 1982) with associated stronger oceanic currents (Sarkar et al, 1990). Furthermore, the South Asian monsoon periods have received much attention as they represent the extremes of planetary scale atmospheric and hydrospheric cycles. In comparison, the monsoon transition periods *viz.* April-June and September-November have not been looked into in detail in spite of the fact that they are the main rainy season for the eastern Africa and feature a short lived but intense upper oceanic jet in the equatorial Indian Ocean (Wrytki, 1973; Hastenrath et al, 1993; O'Brien and Hulburt, 1974). The strongest winds in the equatorial Indian Ocean are during the intermonsoon period (spring & fall) that are called as Indian Ocean Equatorial Westerlies or IEW (Beaufort et al, 1997) in comparison to rest of the Indian Ocean where winds reach their maximum intensity during the SW or NE monsoon. These IEW are result of the Walker circulation and have been found to exhibit positive correlation with Southern Oscillation index, which is supposed to be a measure of the intensity of the Walker circulation/ El Nino events (Hastenrath et al, 1993; Bjerkness, 1969). The Indian summer monsoon is known to be stronger during the periods of high Southern Oscillation phase (Hastenrath et al, 1993; Pant and Parthasarathy, 1981; Rasmusson and Carpenter, 1983; Ropelewski and Halpert, 1987). To study such an important

phenomenon, a core namely SS 3827 G has been raised from the equatorial Indian Ocean that can help in deciphering the past variations in the intensities of the two monsoon periods and oceanic and atmospheric conditions during the intermonsoon periods.

4.2. Core Location:

Core SS 3827 G is a gravity core with a total length of 196 cm. It was recovered during Sagar Sampada cruise number SS152 during 1997 from a water depth of 3118 m and thus represents an open ocean regime. The location is east of Maldives Islands at latitude $3^{\circ}42'N$ and $75^{\circ}54.5'E$ longitude. For further details refer to Table 2.1. The following figure shows its location along with other cores with which it has been compared.

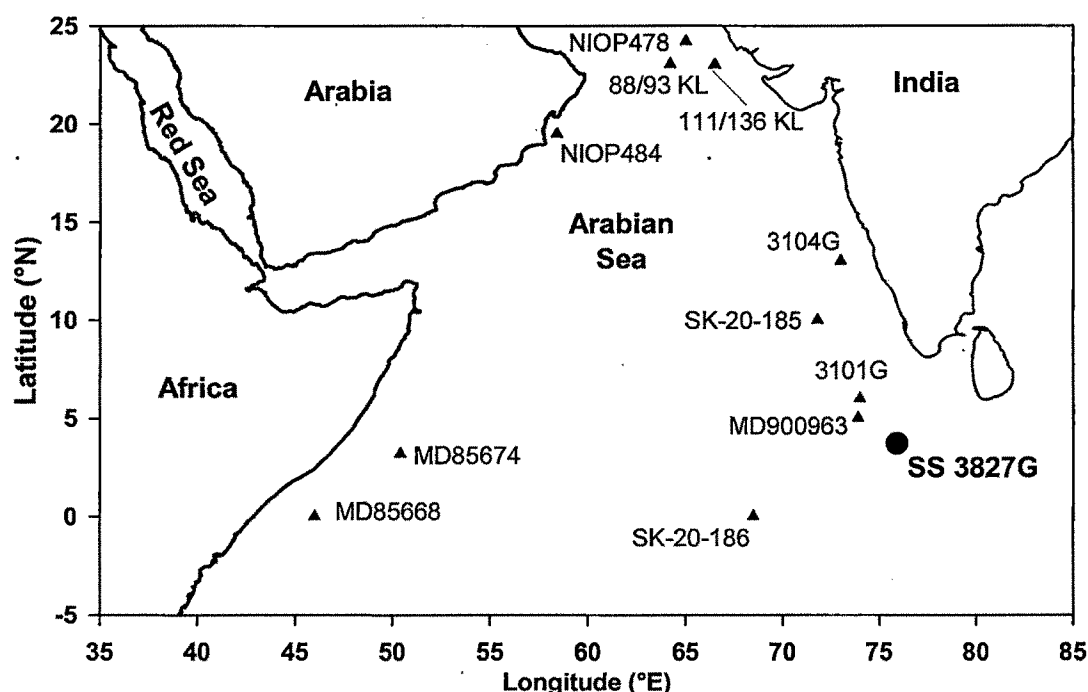


Fig. 4.1. Locations of the core SS3827 G and other cores (depicted by triangles) with which it has been compared.

4.3. Oceanographic and Climatologic conditions at the core site:

A unique wind-forcing pattern occurs over the equatorial Indian Ocean in the form of strong eastward winds during the intermonsoon periods i.e. April to June and October to November (Schott and McCreary Jr., 2001; Hastenrath et al, 1993). These strong Westerlies are called as Indian Ocean Equatorial Westerlies or IEW (Beaufort et al, 1997) that drive short-lived but intense eastward equatorial jets (EEJ), also known as Wyrki jets, in the upper oceanic layers (Wyrki, 1973). Because of EEJ, the mixed layer deepens from ~ 38 m in the east (60°E) to ~60 m in the west ($\sim 90^{\circ}\text{E}$). The currents due to EEJ reach a maximum intensity in the central basin ($70^{\circ}\text{E} - 75^{\circ}\text{E}$), which induces upper oceanic divergence and upwelling in the west and convergence and downwelling in the east with a subsequent gradient in the SST from 26°C in the east to 29°C in the west (Hastenrath et al, 1993). On reaching the eastern end of the basin, the EEJ get reflected in the form of the Rossby waves as well as northward propagating eastern boundary waves. Along the way, the eastern boundary waves generate slowly propagating mid latitude Rossby waves that radiate into Bay of Bengal and the eastern Arabian Sea (Perigaud and Delecluse, 1992; Basu et al, 2000).

During the two different monsoon periods, the core location is dominated by two different currents namely Southwest Monsoon Current (SMC) and the Northeast Monsoon Current (NMC). Please refer to the Fig.1.1 and 1.2 for a schematic diagram of the Indian Ocean circulation during the summer and winter monsoon respectively. During the summer monsoon, one branch of the Somali Current (SC) turns off shore at around 4°N and supplies the eastward flowing SMC. SC supplies most of the water of the SMC but part of its water is contributed by southward flowing West Indian Coast Current (WICC) after circulating around Laccadive Low (LL). After passing Sri Lanka most of the SMC turns northward into the Bay of Bengal, flowing around cyclonic Sri Lanka Dome, which is generated due to local wind stress. In the Bay of Bengal SMC supplies water to the northeastward flowing East Indian Coast Current (EICC). It is unclear whether a second SMC branch radiates further eastward and eventually bends southward to cross the equator. The chances are bleak as the 6°N transport is almost same as carried past Sri Lanka (Schott and McCreary Jr., 2001).

direction twice a year viz. northeastward from February to September with strongest flow during March-April. During the boreal winter (October to January) EICC flows southwestward with its peak in November. Thus during the NE monsoon period EICC contributes low salinity water to the NMC (as shown in Fig.4.2), which in turn supplies water to the then northward flowing WICC after circulating around the Laccadive high (Bruce et al, 1994).

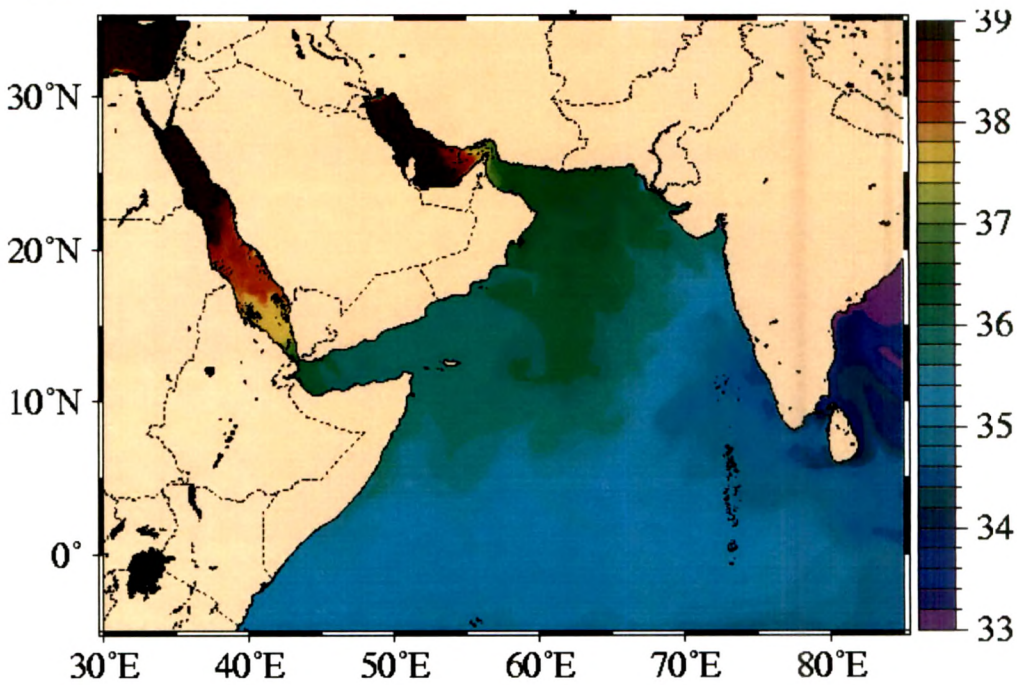


Fig.4.2. The inflow of low salinity water from the Bay of Bengal into the Arabian Sea along the NMC in the month of December. The salinity contours (unit is in PSU) were taken from the website www7320.nrlssc.navy.mil/global_ncom/ara.html.

Another branch of NMC flows westward and meets the southward flowing Somali Current (SC) at around 5°N . SC in turn meets the East African Coast current (EACC) at $\sim 2^{\circ}\text{S}$, which then supplies water to the eastward flowing South equatorial countercurrent (SECC) (Schott and McCreary Jr., 2001).

4.4. Age-Depth Model:

In this core seven AMS dates on planktonic foraminiferal separates, going up to 34,730 calendar years covering the LGM (Last Glacial Maximum; ~21,000 calendar years BP) are available. The total length of the dated core is 100cm. Thus the average sedimentation rate is $\sim 3 \text{ cm}/10^3 \text{ years}$, which is typical of open ocean locations. After 100cm, reversal of the dates was found which is possible if there was a double bounce during coring. The time resolution is approximately 350 years per cm. For dates in tabular form and other related information please refer to Table 2.2.

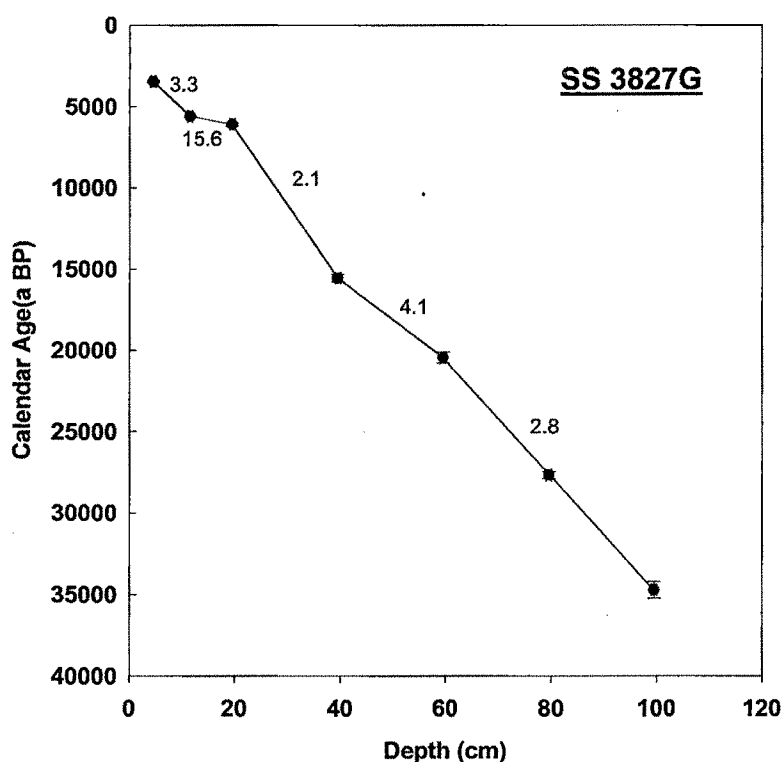


Fig. 4.3. Calibrated Radiocarbon ages and sedimentation rates (cm/ky) for the core SS 3827G.

The radiocarbon dates in this core have been calibrated to calendar ages using the calibration program “Calib 4.1 (INTCAL 98)” (Stuiver et al, 1998) with a reservoir age correction of 500 ± 30 years ($\Delta R = 100 \pm 30 \text{ yr}$, Dutta et al, 2001; see pp 49 for details regarding correction). Southon et al (2002) have reported a ΔR value of

122± 25 yr (weighted mean of the four values) from a location south of Sri Lanka, which is similar to that of Dutta et al (2001).

4.5. Oxygen isotope Analysis:

4.5.1. SW Monsoon vs. NE Monsoon:

Duplessy (1982) studied $\delta^{18}\text{O}$ signatures in the foraminifera *G.ruber* (a surface dwelling species) in 41 piston cores and 36 core top samples from the Arabian Sea, the Bay of Bengal and the Andaman Sea for the Holocene and LGM (Last Glacial Maximum). He found a marked difference in the $\delta^{18}\text{O}$ values for the above two periods that indicated that salinity changed considerably at LGM, which he attributed to reduced river inflow into the Bay of Bengal and increased evaporation in the northern Arabian Sea due to strengthened dry northeastern winds that blew from continents to the ocean. Furthermore, during LGM, the low salinity, low $\delta^{18}\text{O}$ area along the southwestern coast of India (signifying SW monsoon precipitation) and cool, high $\delta^{18}\text{O}$ region along the Arabian coast (signifying upwelling and hence SW monsoon wind strength) also disappeared. Based on these, he concluded that during the LGM southwest monsoon was weaker than today and northeastern monsoon was relatively stronger.

Sarkar et al (1990) obtained a core SK-20-185 from the eastern Arabian Sea (10°N, 71°51'E; for core location refer to Fig.4.1) and measured oxygen isotopes in planktonic foraminiferal species viz. *G.sacculifer*, *O.universa*, *G.ruber* and *G.menardii*. The chronology of the core was obtained by radiocarbon dating on the bulk sediments. They found that all the species exhibited an excursion towards lighter $\delta^{18}\text{O}$ values (by ~1‰) for around 4 kyr centered on LGM. They argued that such a negative excursion can be explained if we consider that during LGM vertical mixing due to SW monsoon reduced considerably resulting in a relative warming by 1-2°C and causing $\delta^{18}\text{O}$ values to become lighter by ~0.3 ‰. More importantly, they proposed that during LGM, NE monsoon winds were stronger that would result in enhanced precipitation (cyclones) over the southeastern India resulting in increased fresh water influx and lower salinities in the southwestern Bay of Bengal. They further argued that Northeast Monsoon Current (NMC) also intensified due to enhanced northeast winds, which brought the low salinity water from the

southwestern Bay of Bengal to the core location resulting in reduction of $\delta^{18}\text{O}$ values by 0.6 ‰ making the total offset to $\sim 1\text{‰}$. They measured $\delta^{18}\text{O}$ in *G.sacculifer* in another core from the equatorial Indian Ocean (0.2°S , $68^{\circ}30'\text{E}$) namely SK-20-186 (for location, refer to Fig.4.1) but did not find any negative excursion during LGM. They explained this observation by maintaining that probably NMC did not reach the core site during LGM (similar to present time oceanographic condition), hence the low salinity waters did not affect this core.

Oxygen isotope analysis was carried out in the core SS 3827G to check the hypothesis of the enhanced inflow of low salinity water into the eastern Arabian Sea along the Northeast Monsoon Current (NMC) during LGM. It should be noted that our chronological control is better than that of Sarkar et al (1990). The core SS 3827G has been strategically chosen from a location that falls well in the way of NMC and is closer to the southwestern Bay of Bengal (see Fig.4.1). If there was indeed a flow of low salinity water along the NMC during LGM, then its signature should be more pronounced in the core SS 3827G. The $\delta^{18}\text{O}$ measurements were carried out in the three species of planktonic foraminifera viz. *Globigerinoides ruber*, *Globigerinoides sacculifer*, *Globorotalia menardii* as shown in the Fig.4.3. *G.ruber* and *G.sacculifer* are surface dwelling species predominantly inhabiting top 25 m and 50 m respectively whereas *G.menardii* is a deeper dwelling species predominantly inhabiting 100-150 m (Be, 1977, Fairbanks et al, 1980; Fairbanks et al, 1982). It is remarkable that all the three species exhibit similar variations inspite of the fact that they dwell at different depths. It indicates that the signals recorded by them are genuine and are corroborated by each other. As evident from the figure 4.3, during LGM ($\sim 21,000$ a BP, calendar age) the $\delta^{18}\text{O}$ values in all the three species of foraminifera exhibit a shift towards heavier values indicating that at the core site there is no influence of low salinity, isotopically lighter water. In fact, during LGM the oxygen isotopes in planktonic foraminifera exhibit most positive values indicating that the temperature was at its lowest with the maximum salinity (due to global ice-volume effect) and least precipitation at the equatorial region. Had there been an enhanced inflow of low salinity water along the strengthened NMC, then it should have been reflected in the oxygen isotopic composition of the planktonic foraminifera, which is not the case. All these evidences point towards the fact that during LGM Northeast Monsoon Current

did not probably strengthen and hence the transport of low salinity water did not probably intensify during that time.

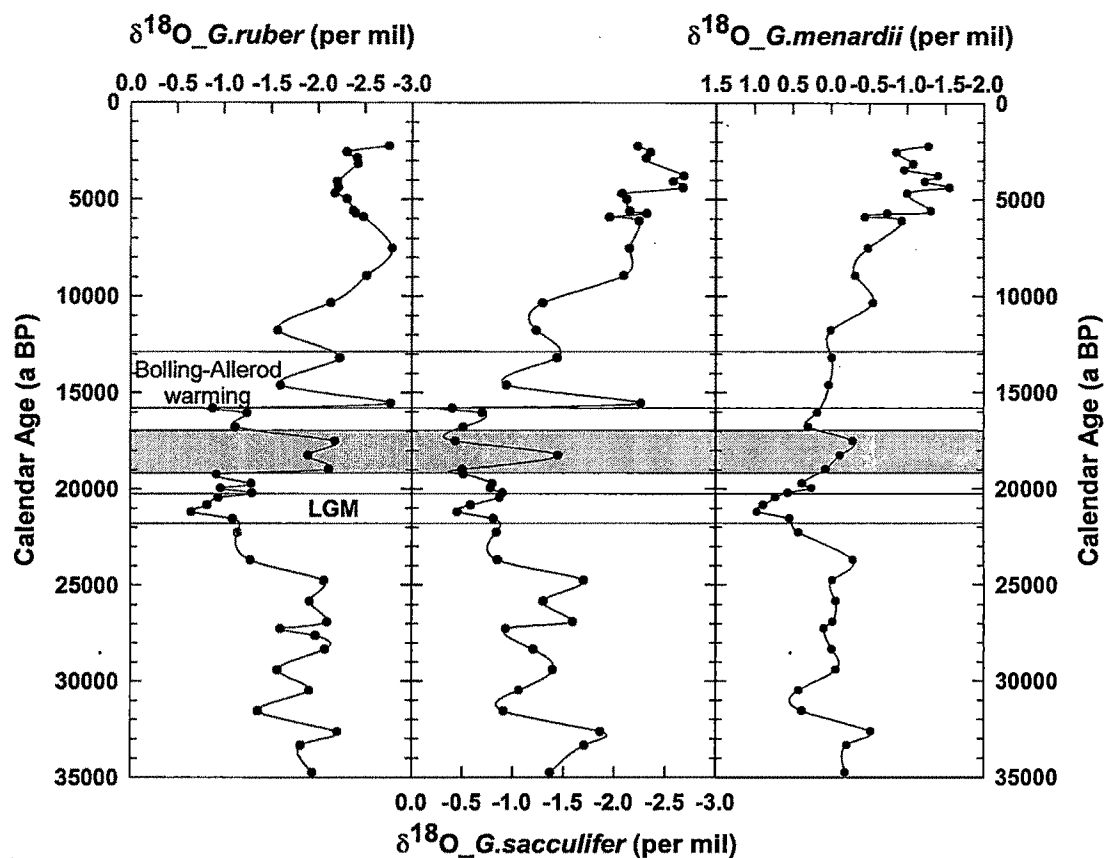


Fig. 4.4. Temporal variations in the oxygen isotope ratios ($\delta^{18}\text{O}$) of three species of foraminifera viz. *Globigerinoides ruber*, *Globigerinoides sacculifer*, *Globorotalia menardii* in the core SS3827 G; negative excursion during early deglacial is shown by shaded region

But then, the question arises as to the signal reported by Sarkar et al (1990). The problem seems to lie in the bulk-dating scheme adopted by them. It has been observed that bulk dating usually yields older ages by a few thousand years because of the contribution by dead carbon due to contamination from detrital carbonate. For example, two cores from adjacent regions namely SS 3268G5 (Sarkar et al, 2000) and SK 145-9 (this study) have been obtained off the coastal southwestern India. In the core SS 3268G5 bulk sediment dating was carried out whereas in the core SK 145-9,

AMS dates have been obtained on the selected species of planktonic foraminifera (see section 3.3). The difference between the bulk dates and AMS dates on planktonic separates might vary depending upon the contribution of the detrital carbonate. So, the signal observed by Sarkar et al (1990) during LGM and lasting for ~ 3000 to 4000 years seems to be the negative excursion in $\delta^{18}\text{O}$ values observed at ~18 ka BP (calendar ages) with a total duration of approximately 3 ka. Thus our study clarifies that the signal seen by the Sarkar et al (1990) is true but the timing of intensification of the NMC is not during LGM but 19ka BP to 17 ka BP (early deglacial period). The core employed in this study is nearer to the southwestern Bay of Bengal (that mainly contributes the low salinity water to the NMC) and possesses better chronological constraints as well as better confidence on results. During that time $\delta^{18}\text{O}$ values decreased by about 1‰ in the surface dwelling *G.ruber* and *G.sacculifer* and by ~0.6‰ in the deeper dwelling *G.menardii* as evident from the Fig.4.3. The $\delta^{18}\text{O}$ decrease due to global ice – volume effect at that time was negligible (0.1‰; Fairbanks, 1989). It has been observed that during SW monsoon the SST in the equatorial region decreased by ~2°C (Wyrtki, 1971) probably due to wind-induced mixed-layer deepening. During the early deglacial SW monsoon was weaker as exhibited by the calcareous and organic productivity indicators and oxygen isotope analysis as discussed in the next chapter (refer sections 5.4.1 and 5.5). Due to reduced mixing the SST would rise by ~2°C that would account for around 0.5 ‰ reduction in $\delta^{18}\text{O}$ values. Moreover, enhanced precipitation would take place over the southeastern India if the NE monsoon was stronger than present. It would result in increased river run off from peninsular India and the SSS (sea surface salinity) in the southwestern Bay of Bengal would reduce further. The remaining ~0.5 to 0.6‰ reduction in the surface dwelling *G.ruber* and *G.sacculifer* can be explained by the enhanced inflow of low salinity water along the enhanced Northeast Monsoon Current (due to enhanced NE monsoon wind strength). If the salinity reduced by ~2‰ it would account for the ~0.6‰ decrease in the $\delta^{18}\text{O}$ values (as in this region for every per mil decrease in salinity $\delta^{18}\text{O}$ values decreases by 0.33‰; Duplessy et al, 1981; Sarkar et al, 2000). Since *G.menardii* is deeper dwelling (~150m; Be, 1977) so it is not affected by the NMC, which is a surface current. The NMC is known to exist upto a depth of ~120m (Schott and McCreary Jr., 2001). Thus the signal exhibited by *G.menardii* only

reflects the relative warming of the sea surface due to slackening of the SW monsoon winds. Many studies based on various paleoclimatic proxies have shown that SW monsoon was relatively weaker than present during the LGM (Prell et al, 1980; Van Campo et al, 1982; Duplessy, 1982; Prell and Van Campo, 1986). It has been further suggested that there are weak oceanic indications of concurrently stronger NE monsoon (Duplessy, 1982). The reason proposed for this observation is that during glacial times Tibetan plateau was covered with glaciers (Singh and Agrawal, 1976). Hence during summer, enough heat was not taken up by Tibetan landmass resulting in a lower land – sea pressure difference because of which SW monsoon winds were weaker. They further proposed that during winter months the land was cooler than present (due to permanent ice cover) in the vicinity of a warm ocean resulting in the relatively stronger NE monsoon. But our study points towards a slightly revised picture. During the LGM, no doubt, the SW monsoon slackened because of permanent ice cover. But the SSTs also fell by 2-3⁰C in the tropical regions (Lea et al, 2003; Kienast et al, 2001; Rosenthal et al, 2003). The outcome was that NE monsoon also weakened along with the SW monsoon. But during early deglacial period the SW monsoon was still in a weakened mode due to presence of considerable ice cover that disappeared only during the Termination IA (T IA). During the early deglacial period there were not much ice melting episodes as evident from the sea level rise of only 15m in ~5000 years (LGM to T IA) whereas in the next 5000 years starting from T IA, the sea level rose by ~75m (Fairbanks, 1989). In contrast the SSTs in the equatorial Indian Ocean and southern tropical Indian Ocean rose during early deglacial period (by ~1⁰C (Bard et al, 1997) that accounts for about 33% of the total LGM to Holocene temperature amplitude) resulting in the enhancement of the NE monsoon. This period of relatively stronger NE monsoon lasted for about ~2000 years starting from ~19 ka BP, which is clearly reflected in the oxygen isotope record.

4.5.2. Correlation with the high latitude temperature record:

The oxygen isotopic values for the equatorial core SS3827 G exhibit a good resemblance with the GISP2 $\delta^{18}\text{O}$ record (Grootes et al, 1993; Stuiver et al, 1995; Grootes and Stuiver, 1997; Meese et al, 1994 a, b) as depicted in Fig.4.4.

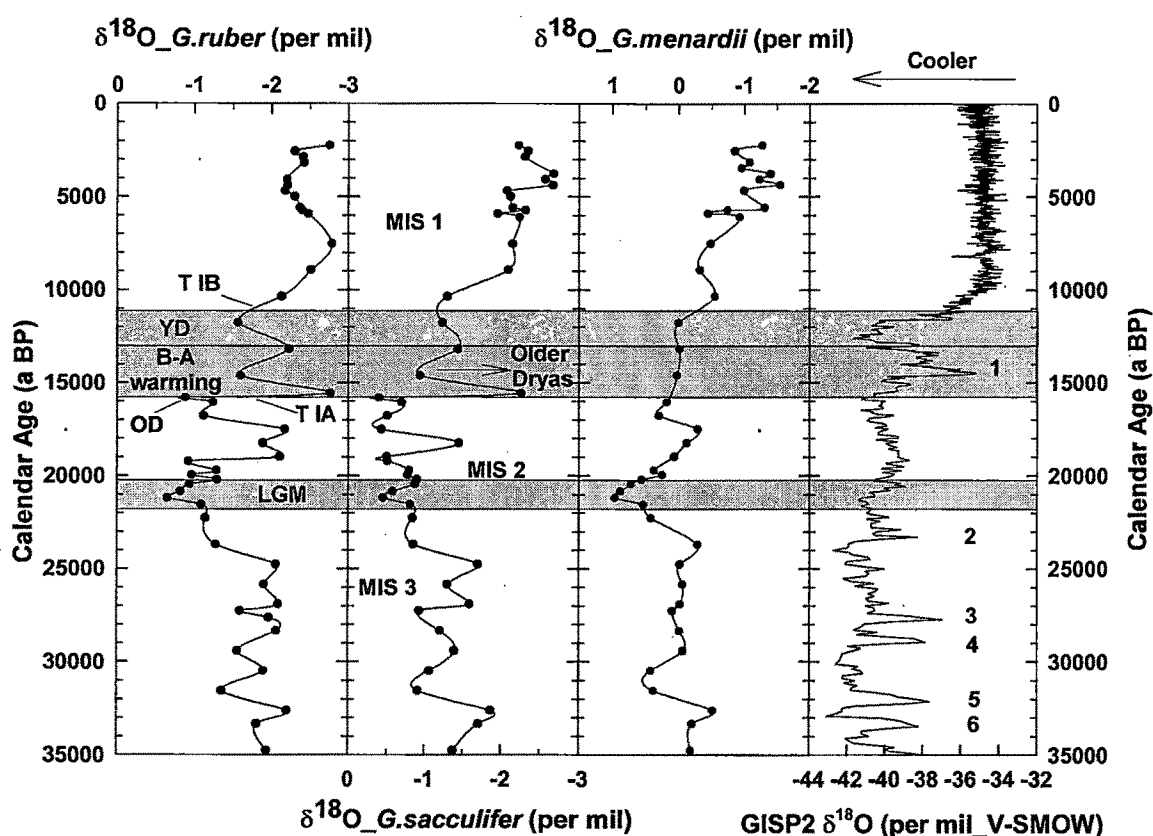


Fig.4.5. Comparison of the $\delta^{18}\text{O}$ record of the core SS3827 G with the GISP2 $\delta^{18}\text{O}$ record; OD, T IA, B-A warming, YD and T IB shown in the first panel refers to Oldest Dryas, Termination IA, Bolling-Allerod warming, Younger Dryas and Termination I B respectively (Stuiver et al, 1995); MIS 1, MIS 2, MIS 3 in the second panel refer to standard SPECMAP (Martinson et al, 1987) Marine Isotope Stages 1, 2 and 3; Arabic numerals in the last panel (1 to 6) indicate Dansgaard/Oeschger Interstadials.

Foraminiferal $\delta^{18}\text{O}$ values respond to sea surface temperature (SST), global change in seawater $\delta^{18}\text{O}$ due to the ice volume effect (sea level change) and local salinity changes due to evaporation – precipitation (E-P) budget. Low sedimentation and bioturbation limit the temporal resolution of sedimentary cores. Furthermore equatorial and tropical regions, by virtue of their distance, are not directly affected by ice sheet behaviour. That is why there are very few studies [e.g. Kienast et al (2001) in the South China Sea; Lea et al (2003) from the Cariaco Basin, northern Venezuelan shelf; Rosenthal et al (2003) from the Pacific] comparing the oxygen isotope analysis of equatorial/tropical sediment cores with ice cores. Bard et al (1997) carried out oxygen isotope and alkenone measurement from two cores viz. MD85674 and MD85668 (see Fig. 4.1) for the past 150 ka BP in the northwest equatorial Indian Ocean. They reported that 70% – 80% of the total ^{18}O signal is due to global ice-volume effect and the LGM to Holocene temperature change is of the order of $\sim 2^{\circ}\text{C}$, which is in marked contrast to $5\text{--}6^{\circ}\text{C}$ deglacial warming inferred from the Sr/Ca ratio in tropical corals (Guilderson et al, 1994). Schulz et al (1998) measured total organic carbon in cores from the northern Arabian Sea namely SO 90-88KL, SO 90-93KL, SO 90-111KL and SO 90-136KL as shown in the Fig.4.1. They found that strong SW monsoon as manifested by organic carbon rich bands corresponded to mild interstadials of the North Atlantic (D/O events) and periods of weak SW monsoon correlated with high-latitude atmospheric cooling and injection of melt water into the North Atlantic basin (Heinrich events). They concluded that such events (D/O and Heinrich) are an important component of low-latitude climate that points towards a large scale element of the ocean-atmosphere system interacting rapidly with the high and low latitudes. They further maintained that interstadials recorded in the ice core records represented periods of global warmth associated with high levels of greenhouse gases as suggested by Mayewski et al (1994) and Brook et al (1994). Reichert et al (1998, 2002 a) measured the C_{org} content in the cores NIOP478 and NIOP484 from the northern and western Arabian Sea (see Fig. 4.1). They found excellent correlation between the low C_{org} values (denoting reduced summer monsoon) during the stadials. Altabet et al (2002) studied the denitrification records from the western Arabian Sea and found that denitrification intensified (denoting more productivity and hence enhanced SW monsoon winds) during periods of polar warmth

as suggested by the $\delta^{18}\text{O}$ data from the GISP2. Rostek et al (1993) estimated the SST for the past 170,000 years in the core MD900963 (location shown in the Fig.4.1) using the alkenone unsaturation ratio. They found that for the past 35,000 years (the studied length of the present core SS3827 G), the SST variation at the core site was within 2.5°C with a minimum at LGM (25.5°C) and a present SST maximum (28°C). In spite of the comparatively poorer resolution [the $\delta^{18}\text{O}$ measurements have been carried out usually at alternate depths or after every 3 cm, (except for some periods such as LGM that were sampled at every cms) that provides a resolution ranging from 700 yrs to 1000 yrs] than the ice core record, we find very good correlation to the extent that even some rapid events like Dansgaard/Oeschger (D/O) Interstadials appear to be reflected in the sediment core oxygen isotope record. Because of the resolution problem many of the peaks observed in the ice core record are merged into one in the sedimentary record. For example the D/O event 5 and 6 are represented by a peak at 32.5 ka BP in all the three species of foraminifera; D/O events 3 and 4 are shown by a peak at 28.5 ka BP (again in all the three species). Similarly the D/O event 2 is represented by peaks at 24 ka BP and a peak at 15 ka BP corresponds to D/O event 1 in all the three species of planktonic foraminifera.

During the MIS (Marine Isotope Stage) 3 (upto 25 ka BP) various millennial scale fluctuations are found in the sedimentary record that correspond quite well with those of the ice record as outlined above. These negative excursions (upto 0.5‰) are observed at 32.5 ka BP and 28.5 ka BP corresponding to the D/O events 5,6 and 3,4 respectively (Fig.4.4). The equatorial Indian Ocean SSTs increased by $\sim 1^{\circ}\text{C}$ from 35 ka BP to 25 ka BP (Rostek et al, 1993) before plunging back to LGM levels and global seawater $\delta^{18}\text{O}$ first decreased and then increased by 0.2‰ in the 10 ka (Labeyrie et al, 1987). But these long-term changes will not have much bearing on the short term, high frequency fluctuations. Thus these millennial scale fluctuations can be only be explained by changes in the evaporation – precipitation (E-P) balance. Enhanced precipitation can shift the $\delta^{18}\text{O}$ values towards the negative side. Since precipitation over Indian Ocean is related to the strength of the SW monsoon (Cadet and Reverdin, 1981; Rostek et al, 1993), it can be deciphered that negative excursions coinciding with the North Atlantic interstadials reflect an increase in the precipitation over equatorial Indian Ocean.

From 25 ka BP to LGM the oxygen isotope values show an increase of about 1.5‰ in all the three foraminiferal species. During that period the temperature plummeted by 1.5°C (Rostek et al, 1993) that would account for the ~0.3‰ to ~0.4‰ (considering a slope of 0.25‰ rise in foraminiferal $\delta^{18}\text{O}$ for every °C fall in temperature; Erez and Luz, 1983) enhancement in foraminiferal $\delta^{18}\text{O}$ and global seawater $\delta^{18}\text{O}$ increased by 0.6‰. These two effects will account for the ~1‰ increase in the $\delta^{18}\text{O}$ values. The remaining ~0.5‰ increase is due to the reduced precipitation, which points towards the fact that during LGM the precipitation at the equatorial Indian Ocean reduced considerably corroborating many of the earlier studies that were carried out in the western Arabian Sea (Prell et al, 1980; Van Campo et al, 1982; Duplessy, 1982; Prell and Van Campo, 1986). The maximum $\delta^{18}\text{O}$ signal is obtained for the LGM signifying that during that time precipitation was at its minimum corresponding exactly with the maximum global glaciation.

After LGM, during early deglaciation we find a negative excursion by ~1‰, which is due to the effect of relatively enhanced NE monsoon as discussed in the previous section (Sec.4.5.1). The transition from glacial to Holocene is punctuated with numerous fluctuations in the foraminiferal $\delta^{18}\text{O}$ record that are synchronous with those occurring in the GISP2 record within the dating errors and the core resolution. At around 15.7 ka BP an increase by 0.5‰ in the $\delta^{18}\text{O}$ values is found for the sea surface dwelling species (*viz.* *G.ruber* and *G.sacculifer*) that probably corresponds to the cold “Oldest Dryas” observed in the GISP2 record (Stuiver et al, 1995) indicating that precipitation reduced during that time. This signal was not observed for the *G.menardii*, which is the deeper dwelling species (~150 m water depth). It is interesting that $\delta^{18}\text{O}$ values in *G.menardii* do not show rapid fluctuation as in the case of other two species during the late deglaciation period (16 ka BP – 11 ka BP). In the case of *G.menardii*, the $\delta^{18}\text{O}$ values just exhibit an uniform increase by ~0.7‰, which is the global ice-volume effect during the late deglaciation. This clearly indicates that during this time the precipitation variation was not as strong as glacial times when it affected the depths at which *G.menardii* dwells. At 15.5 ka BP we observe a rapid decline in the $\delta^{18}\text{O}$ values by ~1.7‰ in surface dwelling species which corresponds to the Termination IA (T IA), and the GISP2 $\delta^{18}\text{O}$ record. During this event the

equatorial SST increased by roughly 1°C (Rostek et al, 1993) and the global seawater $\delta^{18}\text{O}$ decreased by $\sim 0.35\text{‰}$ that would account for nearly 0.6‰ reduction in $\delta^{18}\text{O}$. The remaining 1‰ depletion has to be explained by some other process. Out of that around 0.4‰ can be attributed to precipitation increase due to SW monsoon enhancement. But it can't be more than 0.4‰ because the precipitation fluctuations are weaker than what was during glacial times as reasoned above. The remaining 0.6‰ decrease can be explained if we take into account the fact that during TIA, surface temperature increased that would cause the Himalayan glaciers to melt. This along with the enhanced SW monsoon precipitation would result in greater fresh water runoff as rivers in to the Bay of Bengal. The influx of water with salinity lower by upto 2‰ at the core site via the Northeast Monsoon current would result in the reduction of foraminiferal $\delta^{18}\text{O}$ by upto 0.6‰ (as in the eastern Arabian Sea, foraminiferal $\delta^{18}\text{O}$ values are assumed to decrease by 0.33‰ for every ‰ decrease in salinity, Sarkar et al, 2000). But this influx of low salinity water was not as strong as that during the early deglacial period because deeper dwelling *G. menardii* was not affected.

The Bolling-Allerod (B-A) warming is manifested by depleted $\delta^{18}\text{O}$ values from 15.5 ka BP to 13 ka BP. These values shows that precipitation increased during the warm periods observed in ice core records. Centered at 14 ka BP between the B-A interstadial is the "Older Dryas", a cold period that represents a rapid deterioration in the north Atlantic climate. It is recorded in the foraminiferal $\delta^{18}\text{O}$ values in the form of a sudden increase by $\sim 1\text{‰}$. This sudden enrichment in the oxygen isotopic values reflects the reduction in SW monsoon precipitation that would account for about 0.4‰ . This would reduce the river runoff to the Bay of Bengal with consequent increase in the salinity, which might affect the core site accounting for the remaining 0.6‰ enhancement.

The "Younger Dryas" in the sedimentary oxygen isotope record is represented by an enhancement in $\delta^{18}\text{O}$ values by $\sim 0.4\text{‰}$ in the *G. ruber* and *G. sacculifer* from 13 ka BP to 11 ka BP. During that period the SST reduction in the equatorial region was negligible ($\sim 0.2^{\circ}\text{C}$; Rostek et al, 1993; Bard et al, 1997) and the global seawater $\delta^{18}\text{O}$ decrease was by $\sim 0.15\text{‰}$ (Fairbanks, 1989). Thus the total enhancement in the $\delta^{18}\text{O}$ values would have been by approximately 0.5‰ that could be explained by a

reduction in the SW monsoon. Thus we find that the one of the major North Atlantic cold period, the signature of which have been recorded all over the globe, is conspicuously reflected in the SW monsoon as well.

At the end of YD we find a rapid decrease in the $\delta^{18}\text{O}$ values by $\sim 0.5\text{‰}$ representing the Termination IB (T IB). During that time SST increased by 0.8°C in the equatorial Indian Ocean (Rostek et al, 1993; Bard et al, 1997) that would account for $\sim 0.2\text{‰}$ enhancement in $\delta^{18}\text{O}$ values. During the same time global seawater $\delta^{18}\text{O}$ value reduced by 0.2‰ (Fairbanks, 1989). These two processes would account for most of the signal with the remaining decrease being explained by increasing precipitation.

During the Holocene, which is a period of uninterrupted warmth, the $\delta^{18}\text{O}$ values exhibit a decreasing trend upto the core top ($\sim 2,200$ years) in the *G.sacculifer* and *G.menardii*. The total decrease is about 1‰ out of which around 0.4‰ is accounted by the global seawater $\delta^{18}\text{O}$ decrease and 0.1‰ is due to $\sim 0.5^{\circ}\text{C}$ rise in equatorial SST (Rostek et al, 1993). The remaining $\sim 0.5\text{‰}$ can be explained by an increasing SW monsoon precipitation. *G.ruber* exhibits a decreasing trend upto ~ 7 ka BP after which it shows increase in $\delta^{18}\text{O}$ values for the next 3 ka and then it shows decreasing trend upto core top (2.2 ka). In the Late Holocene (after 5 ka), there are many fluctuations in sedimentary record that seem to have a local origin such as centennial scale variations in precipitation. But they are not found in the polar record. Similarly, the prominent 8,200 a BP cold event in the GISP2 record does not seem to have a counterpart in the present sedimentary record.

Notwithstanding resolution problems, it appears that SW monsoon correlates very well to the North Atlantic climate, represented by the GISP2 $\delta^{18}\text{O}$ record. The nearly similar variations observed in three different species of foraminifera gives confidence to this. Even the rapid events like D/O events, T IA, T IB, Oldest, Older and Younger Dryas are well recorded in the sedimentary record within the restraints put by the dating errors and the sampling resolution. Such a good correspondence with the North Atlantic climate necessitates for a mechanism that would control both the high latitude and low latitude climate on timescales much shorter than a millennium. It appears that synchronous changes in the equatorial and North Atlantic climate indicate that low latitude played an important role in modifying the high

latitude climate via atmospheric forcing. It is possible that tropical/equatorial regions were instrumental in putting high amount of tropospheric moisture and greenhouse gases such as methane during the interstadials, which acted as a positive feedback mechanism (e.g. Schulz et al, 1998; Altabet et al, 2002; Mayewski et al, 1994).

4.6. Temporal Variations in Productivity:

Various proxies were measured to decipher the past variation in the productivity at the core site, which includes calcium carbonate content, organic carbon percentage, stable isotope of nitrogen ($\delta^{15}\text{N}$) in the sedimentary organic matter along with $\delta^{13}\text{C}$ in the three different species of planktonic foraminifera.

4.6.1. Productivity as Exhibited by Calcium Carbonate Content:

Calcareous productivity was estimated by determining the total carbonate content in a given weight of sediment expressed in percent as shown in the Fig.4.6. Since the core location is well away from land i.e. in the open ocean, terrestrial input is negligible and calcareous productivity observed at the core site is likely to be of marine origin.

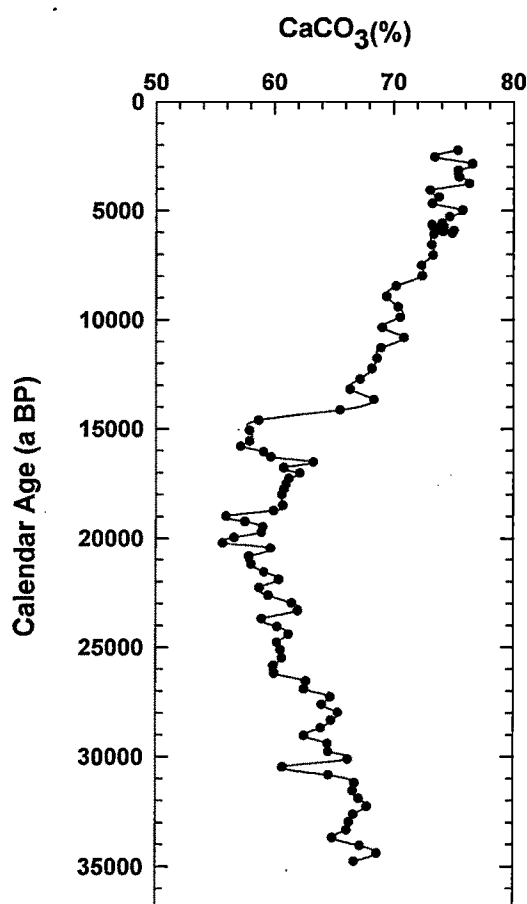


Fig.4.6. Downcore variation of CaCO_3 (%) in the core SS3827 G for the past 35 ka.

In this core calcium carbonate percentage varies from 55% to 75% with a minimum during LGM and a present maximum value. The productivity in the open equatorial Indian Ocean at the core site is due to the wind stress (Beaufort et al, 1997). The wind induced mixed layer deepening would cause the deeper nutrient rich water to surface that would cause the productivity to increase. In this region winds are strongest during April to November with maximum variability during the monsoon transition periods viz. April to June and October to November that are called as Indian Ocean Equatorial Westerlies or IEW as discussed in the section 4.3 that cause short-lived but intense eastward upper ocean water currents called Eastward Equatorial Jets (EEJ) (Wrytki, 1973; Schott and McCreary Jr., 2001; Hastenrath et al, 1993; Beaufort et al, 1997). The strong variability during the monsoon transition period is the result of strong wind bursts capable of causing deeper mixing of the surface water to the effect that maximum productivity in this region occurs during the intermonsoon periods (McIntyre and Molino, 1996; Beaufort et al, 1997). Thus the productivity variation at the core site is a proxy for the strength of IEW. The IEW in turn is positively correlated to Southern Oscillation (SO) index (Hastenrath et al, 1993) and the Walker Circulation with implications to ENSO (El Nino–Southern Oscillation) variability (El Nino tends to occur in the low SO phase e.g. Reverdin et al, 1986; Hastenrath et al, 1993). If so, the equatorial Indian Ocean productivity records should exhibit a correlation with the eastern equatorial Pacific productivity records. In fact Beaufort et al (1997) have shown that the Maldives primary productivity-insolation phase is similar to that of the Pacific primary productivity records in the precession band indicating the influence of SO on both regions on a millennial timescale. Eastern Africa possesses two rainy seasons. The first, which is more abundant in terms of rainfall, occurs during the March to June with its core around April-May (called as “long rains” in Kenya and “Gu” rains in Somalia). The second occurs from September to November, which exhibits more interannual variability in the precipitation, with its core around October-November (called as “short rains” in Kenya and “Der” rains in Somalia). High correlation of these rainfalls with the SO phase have been reported by various authors. During high SO phase enhanced “long rains” have been found by authors like Hastenrath et al (1987); Bhatt (1989); Beltrando and Camberlin (1993);

Ogallo et al (1998) and strengthened “short rains” have been found by Van Heerden et al (1988); Martarira (1990) and Walker (1990). El Nino affects the Indian monsoon in the way that the rising limb of the Walker circulation and the tropical convection, which is usually located in the western Pacific shifts towards the central and eastern Pacific. It would result in subsidence over the western Pacific and the Indian subcontinent, which suppresses convection and precipitation over the Indian landmass (Pant and Parthasarthy, 1981; Rasmusson and Carpenter, 1983; Ropelewski and Halpert, 1987). The high SO phase is related to a low El Nino activity and hence strengthened Indian SW monsoon (Hastenrath et al, 1993). Thus past variation in the intensity of IEW can illuminate the past fluctuations in the El Nino/Southern Oscillation index, Indian summer monsoon and east African rainy seasons.

The calcareous productivity at the core site exhibits a decreasing trend upto LGM (~21 ka BP; calibrated age) as shown in the Fig.4.5, which points towards the uniformly decreasing strength of the IEW. At LGM we find the minimum calcareous productivity signifying the minimum IEW strength. It implies that at LGM the Southern Oscillation index was at its minimum, which indicates that at that time Walker circulation weakened considerably. The low SO index further indicates that SW monsoon as well as the east African rains weakened gradually upto LGM with their minimum values at LGM.

Thereafter the calcareous productivity shows a slight increase from LGM to 16.5 ka BP, which coincides with the early deglacial period. After that it suffered a decline for the next 1000 years falling back to LGM values indicating that IEW strength reduced considerably during that time which implies a lower SO phase i.e. reduced SW monsoon and east African rains at that time. Thereafter a sharp increase in the calcareous productivity was found at ~14.5 ka BP, which coincides with the Termination IA, as also recorded in the Greenland ice cores. This points towards enhancement of SW monsoon and east African rains during that time along with a decrease in the El Nino events. A similar trend in the calcareous productivity with a decline during the late deglacial period and a sudden increase at ~15 ka BP was also observed in the core from the western Arabian Sea (SS 4018 G; this study, Chapter-5), which indicates SW monsoon intensification at that time. Till then to the core top (2.2 ka BP) the productivity shows a steadily increasing trend implying a

strengthening Walker Circulation, which means strengthening SW monsoon, east African rains and lower El Nino frequency during the Holocene.

4.6.2. Regional climatic evolution: comparison with eastern Arabian Sea:

The calcareous productivity record of the SS 3827G was compared with other calcareous productivity records to further explore the regional climatic conditions in the eastern and southern Arabian Sea. Agnihotri et al (2003 a) analyzed two cores from the eastern Arabian Sea viz. SS3104 G and SS 3101 G (location shown in the Fig.4.1) from the water depths of 1680 m and 2680 m. The chronologies of the cores were obtained by AMS radiocarbon dating on the selected planktonic foraminifera species. They attributed the productivity variation to the variation in the SW monsoon wind strength. The following figure compares the productivity variations in the three cores for the past 35 ka.

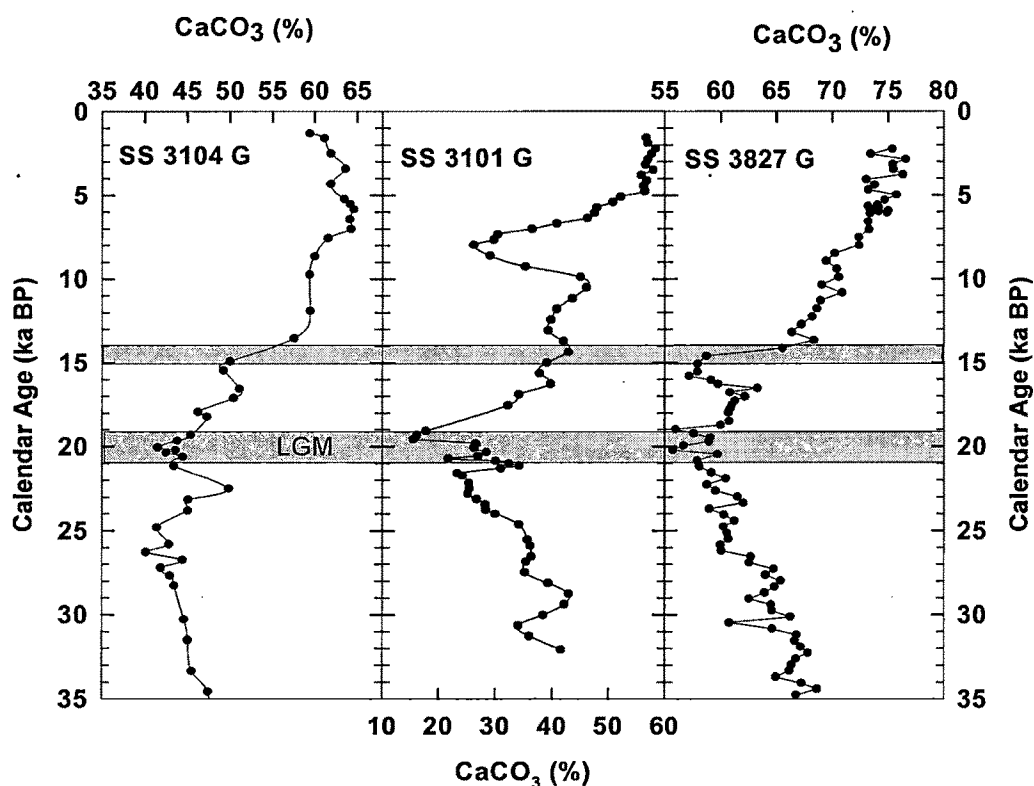


Fig. 4.7. Comparative study of the core SS3827 G (last panel; this study) with other cores from eastern Arabian Sea viz. SS3104G and SS3101G (Agnihotri et al, 2003 a).

All the three cores exhibit more or less similar downcore variations in calcareous productivity, which shows a decreasing trend upto LGM (shown by the

shaded region) from 35 ka BP. It implies that both the SW monsoon winds as well as the Indian Ocean Equatorial Westerlies (IEW) declined in tandem upto LGM pointing towards the fact that the same forcing factor (insolation) is governing both of them. Thereafter around 14.5 ka BP another episode of SW monsoon winds and IEW strengthening are observed as indicated by sharp increase in the calcareous productivity at that time. During the Holocene all the cores show more or less increasing trend in the calcareous productivity except for the core SS3101 G that suffers an abrupt decline during 7-9 ka BP. This abrupt decline is quite intriguing, as it is not observed in the cores north and south of it. It clearly points towards some local effect that dominates the productivity signal. Agnihotri et al (2003 a) explained that timing of this decline coincides with the Holocene humid interval, which is a period of intensified SW monsoon in the Arabian Sea (Sirocko et al, 2000). They speculated that this sharp decline could be due to the build up of low salinity cover due to influx of fresh water from the coastal regions that would inhibit upwelling and hence reduce the productivity (Thamban et al, 2001).

Thus based on the comparative analysis of these three cores we can infer that the productivity trends in the eastern and southern Arabian Sea were similar (apart from some local effects), which points towards the fact that IEW as well as SW monsoon winds strengthened and weakened in synchronicity, implying a common forcing factor.

4.6.3. Productivity as exhibited by Sedimentary Organic Matter:

The core SS3827 G is from a open ocean location from a water depth of 3118 m. Schulte et al (1999) have shown that the equatorial Indian Ocean near the core site of SS3827 G has remained under oxic conditions for the past 330 ka. The C_{org} (%) is a traditional proxy for the organic productivity (Muller and Suess, 1979; Rixen et al, 2000; Ganeshram et al, 1999) but because of the prevailing oxic conditions the preservation of organic carbon in the present core is very poor as shown by the very low values of C_{org} with most of the values being less than 0.5% and in many cases even less than 0.1%. The organic carbon content (C_{org} %) has been obtained by subtracting the inorganic carbon values estimated from the $CaCO_3$ (%) from the total carbon values as discussed in the section 2.5.2. When the organic carbon content is

very low then the total carbon is essentially reflected by the inorganic carbon content of the CaCO_3 . Subtracting the inorganic carbon from the total carbon content to obtain the organic carbon will yield an C_{org} variation that exhibits an exact anticorrelation with the CaCO_3 variation as shown in Fig.4.7.

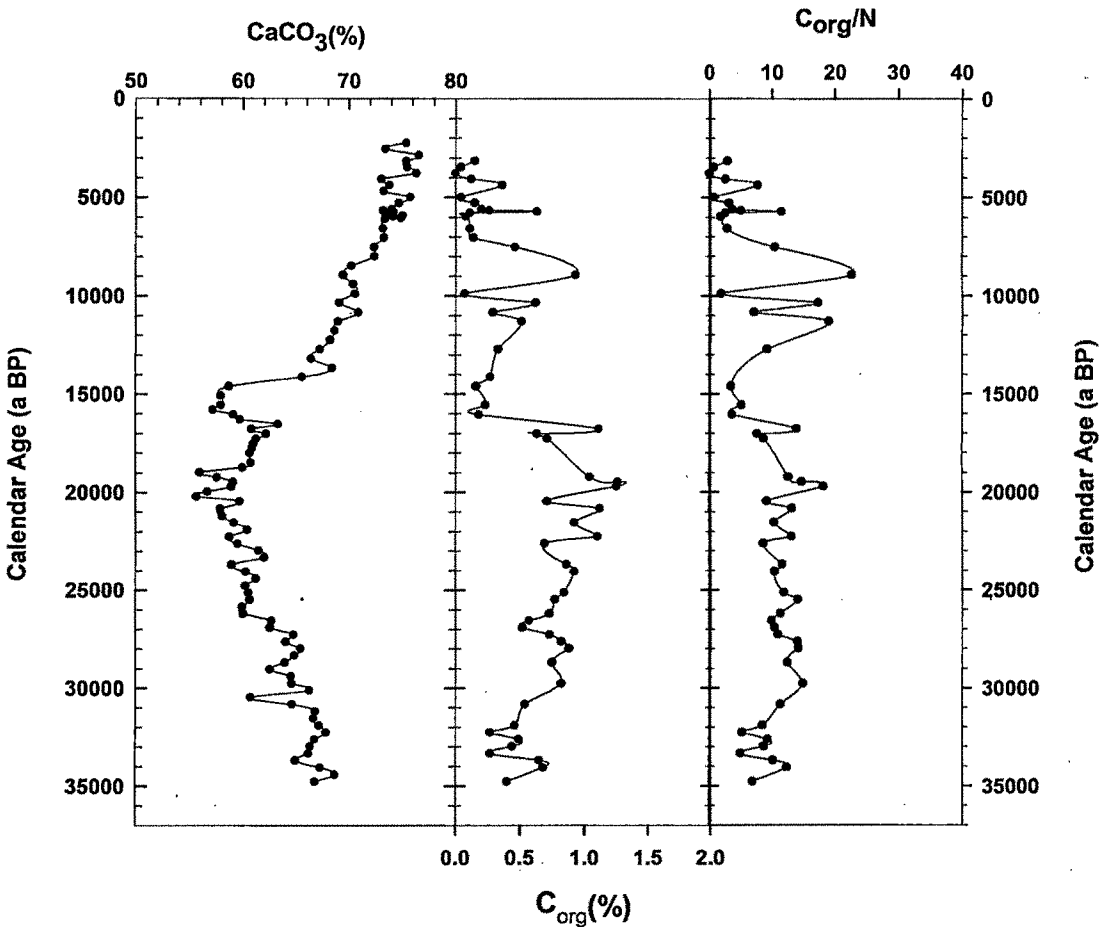


Fig.4.8. Downcore variations in C_{org} plotted along with CaCO_3 (%) and C/N ratio

C/N ratio is obtained by dividing the organic carbon content (C_{org}) with nitrogen content of the sedimentary organic matter that is again very low with a typical value of $\sim 0.04\%$ and has stayed more or less same throughout the core. Therefore the C/N ratio also exhibits a fluctuation similar to the C_{org} variations. Thus this method of determining C_{org} can't be used in the regions with such a low organic carbon content, which may be either due to poor preservation or due to low overhead productivity. In such cases C_{org} cannot be used reliably as a productivity indicator.

4.6.4. Productivity as exhibited by $\delta^{15}\text{N}$:

Denitrification is known to occur in the oxygen deficient waters and is ultimately controlled by the overhead productivity (Deuser et al, 1978; Naqvi, 1991). The $\delta^{15}\text{N}$ of the sedimentary organic matter has been used as a proxy for the water column denitrification (Altabet et al, 1995, 1999; Ganeshram et al, 1995; Agnihotri et al, 2003 b). Near the core site, oxygen deficient conditions are known to exist between 100 to 200 m and then between 500 to 1000 m with the O_2 levels falling to ~ 1 ml/l (Schulte et al, 1999). $\delta^{15}\text{N}$ of the sedimentary organic matter has been measured in the core SS3827 G to explore the possibility of productivity induced denitrification in the water column. The $\delta^{15}\text{N}$ values exhibit very wide fluctuations without any trend as shown in Fig.4.8.

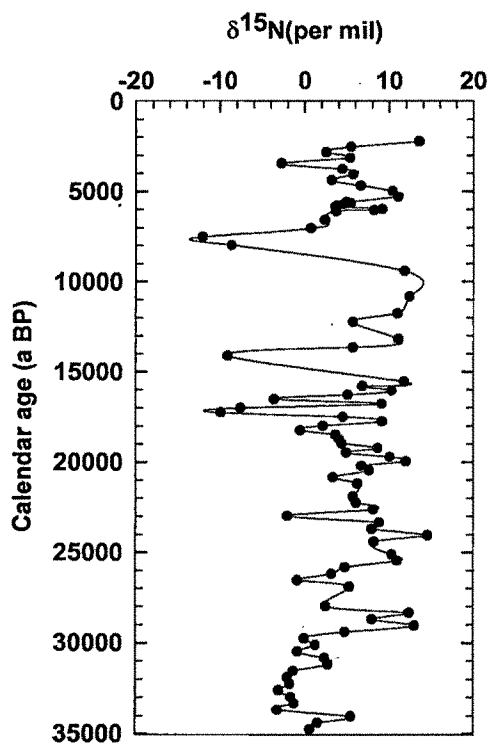


Fig.4.9. Downcore variation of $\delta^{15}\text{N}$ in the core SS3827 G for the past 35 ka.

The reason for such a behaviour by $\delta^{15}\text{N}$ in this core is the low amount of sedimentary nitrogen present. As discussed above in the section 4.6.2, the percentage of sedimentary organic matter is very low. Because of low organic matter and hence low nitrogen percentage the measurement of $\delta^{15}\text{N}$ could not be performed satisfactorily as nitrogen content was less than the range for which the mass spectrometer behaviour is linear. To test this, the $\delta^{15}\text{N}$ values for all the three cores

analyzed in this study were plotted with respect to the respective nitrogen content as shown below in the figure 4.10.

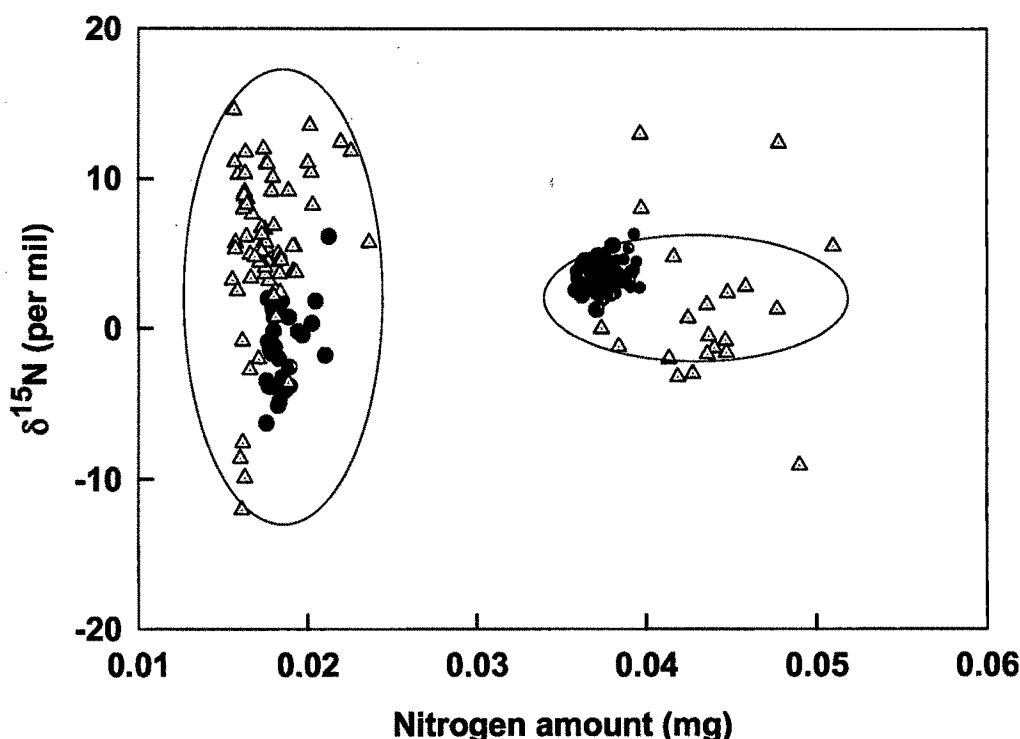


Fig.4.10. $\delta^{15}\text{N}$ vs. Nitrogen content (in mg) for all the three cores viz. SS3827 G (green triangle), SS4018 G (blue circle) and SK 145-9 (red circle) analyzed in this study.

There are clearly two clusters of the data points corresponding to different amount of nitrogen content. As evident, when the nitrogen content of the sedimentary sample is sufficient (>3.5 mg) then the $\delta^{15}\text{N}$ values vary between very small range and fall well within the linear range of the mass spectrometer. On the other hand, when the nitrogen content is less (<2 mg, approximately) then the $\delta^{15}\text{N}$ values fluctuate widely, clearly getting out of the range along which mass spectrometer exhibits linear behaviour. Most of the data points in the cluster showing wide variation in the isotopic values belong to the core SS3827 G. We conclude that $\delta^{15}\text{N}$

values are not useful as a productivity indicator in this case because of the very low amount of sedimentary organic matter/ nitrogen content present.

4.6.5. Productivity as exhibited by carbon isotopes:

The carbon isotopic values ($\delta^{13}\text{C}$) of planktonic foraminifera are known to be controlled by the $\delta^{13}\text{C}$ of the bicarbonate ions present in the seawater as discussed in the section 2.4.2. The $\delta^{13}\text{C}$ of the bicarbonate ions in turn is controlled by the organic productivity and the $\delta^{13}\text{C}$ of the water coming from below e.g. due to wind induced mixed layer deepening or upwelling. The $\delta^{13}\text{C}$ was measured in the three different species of foraminifera viz. *Globigerinoides ruber*, *Globigerinoides sacculifer*, *Globorotalia menardii*, as shown below in fig. 4.10.

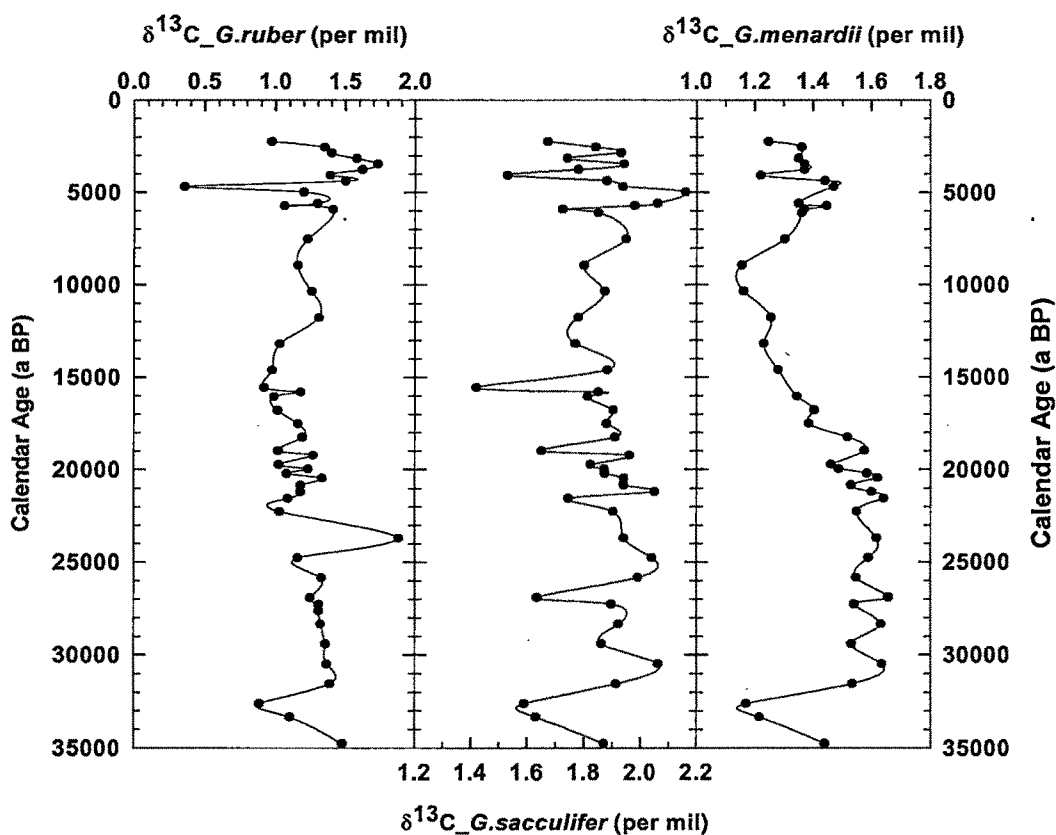


Fig. 4.11. Downcore variation of $\delta^{13}\text{C}$ values of the three species of planktonic foraminifera in the core SS3827 G.

As evident from the above figure the $\delta^{13}\text{C}$ values of any of the three species do not exhibit any trend shown by calcareous productivity such as minimum productivity

at LGM with a sharp increase at ~15 ka BP. One possible reason for such a behaviour by $\delta^{13}\text{C}$ is that it is governed by two competing processes i.e. productivity and upwelling. During enhanced winds, productivity increases due to the influx nutrients from below resulting in the consumption of more of the ^{12}C by the phytoplanktons thus increasing the $\delta^{13}\text{C}$ of the seawater. But the enhanced winds also enhance upwelling and bring the water from the deeper level, which is depleted in $\delta^{13}\text{C}$ (e.g. typically water from a depth of 100 m are depleted by 0.5‰ with respect to surface values, increases to 1‰ by ~600m; Kroopnick, 1985). This upwelled water depleted in $\delta^{13}\text{C}$ essentially negates the enrichment due to productivity and thus reduces the signal. The core site falls in the equatorial upwelling zone and is also influenced by the wind induced mixed layer deepening. When due to stronger winds productivity is higher then surface layer mixing and upwelling are also higher resulting in a mixed signal as discussed above. The $\delta^{13}\text{C}$ can be used as a productivity signal in those regions only where the productivity signal is so strong that it masks the upwelling effect e.g. in the western Arabian Sea.

4.7. Spectral Analysis:

Spectral analysis has been carried out on the time-series data of various proxies to detect the underlying inherent periodicities that might point towards the various forcing factors governing the climatic condition at the core site. The proxies that were analyzed included $\delta^{18}\text{O}$ in all the three species of foraminifera viz. *G.ruber*, *G.sacculifer* and *G.menardii* along with the $\text{CaCO}_3\%$ using the REDFIT 3.6 program (Schulz and Mudelsee, 2002). Proxies such as C_{org} content and $\delta^{15}\text{N}$ in the sedimentary organic matter were excluded from this exercise as their variations do not truly represent the changes in overhead productivity because of their low content as discussed in the section 4.6.2 and 4.6.3. Similarly $\delta^{13}\text{C}$ in foraminiferal species were not analyzed, as their variations are the mixed outcome of two processes i.e. productivity and upwelling, which tends to confuse the signal. The various spectra that were obtained are shown in Fig.4.11.

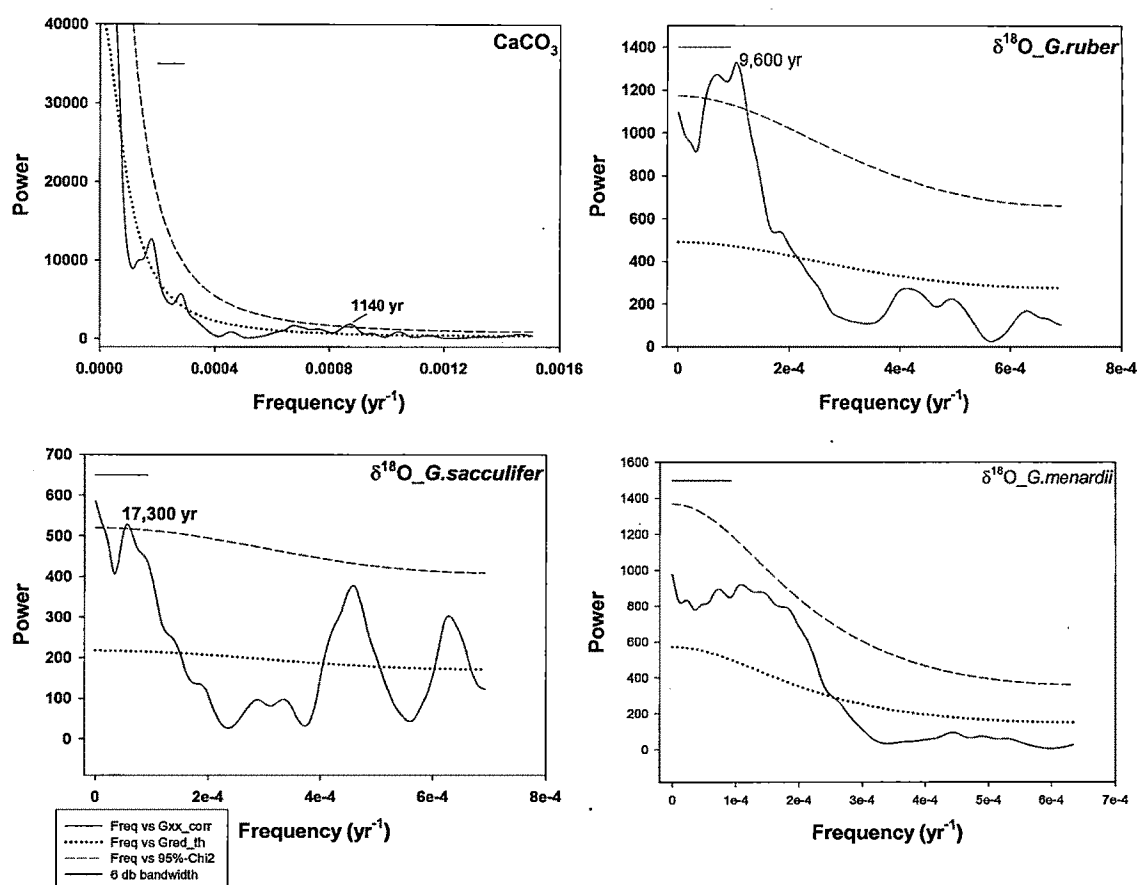


Fig.4.12. Power spectra for various paleoclimatic proxies. Horizontal line at the upper left-hand corner represents 6db bandwidth of the spectral resolution. Gxx_corr denotes amplitude or power of various frequencies; Gred_th shown by dotted line is the background signal; dashed line denotes the 95% significance level calculated using the χ^2 test.

$\delta^{18}\text{O}$ spectrum of the foraminiferal species *G.sacculifer* is dominated by the 17,300 years (y) periodicity, which is very close to the 19,000 y cycle observed for the Earth's precessional cycle. Various other workers like Clemens et al (1991), Rostek et al (1997), Reichert et al (1997), Leuschner and Sirocko (2003) have proposed that in the tropics precessional phase (~ 23 ky) dominates the SW monsoon and associated phenomenon. For example Reichert et al (2001) have shown that C_{org} spectrum is dominated by the 23 ky periodicity while Ti/Al shows both 100 ky and 23

ky periodicities. Beaufort et al (1997) have noticed that the primary productivity record from the equatorial Arabian Sea in the core MD 900963 is strongly dominated by the precession cycles of the 23- to 19 ky periods. This led them to propose that the productivity variation at the core site is mainly governed by the insolation. The $\delta^{18}\text{O}$ spectrum of the *G.ruber* also exhibits a periodicity of $\sim 9,600$ y, which seems to be a sub-cycle of the 19 ky precession cycle. It points towards the fact that SW monsoon (as $\delta^{18}\text{O}$ variations are mainly governed by the evaporation – precipitation budget) is mainly governed by the insolation variations induced by the precessional cycle of the Earth's orbit.

Time series analysis of the CaCO_3 data exhibits a significant periodicity of ~ 1140 y, which is similar to the 1470 ± 500 y periodicity observed in records from different locations around the globe (e.g. Sirocko et al, 1996; Bond et al, 1997; Schulz et al, 1998; Mayewski et al, 1998, Campbell et al, 1998; Sarkar et al, 2000 Agnihotri et al, 2003b). Grootes and Stuiver (1997) have shown that this 1470 y cycle is exhibited by the Dansgaard – Oeschger events in the Greenland ice core's $\delta^{18}\text{O}$ record i.e. D-O events occur every ~ 1400 y. Similar periodicity observed in our equatorial record points towards a common forcing factor, which appears to corroborate a common link between the tropical and north Atlantic climate. Time series analysis of the $\delta^{18}\text{O}$ in *G.menardii* does not yield any periodicity that might be due to the fact that this species dwells in the deeper water and hence is mildly affected by E-P budget, which mainly controls the $\delta^{18}\text{O}$ variations at the core site. It is also not clear why the spectra of *G.sacculifer* and *G.ruber* differ. One possibility is that their abundance peak at different seasons in this site.

4.8. Inferences:

- i. The NE monsoon did not strengthen during the LGM as proposed earlier based on the bulk dating methods. In fact it intensified during the early deglacial period from ~ 19 ka BP to ~ 17 ka BP as shown by our study on three different species of planktonic foraminifera with better age control.
- ii. Oxygen isotope values of all the three species of foraminifera exhibit a good correlation with the GISP2 $\delta^{18}\text{O}$ record on centennial to millennial timescales.

The warm interstadial periods are accompanied by stronger SW monsoon and cooler stadials correspond to reduced SW monsoon. Although during the Holocene, the correlation was not as good.

- iii. The similar variations observed in the tropical/equatorial climate and the North Atlantic climate indicates that tropics were instrumental in bringing about high latitude climatic changes, most probably via atmospheric forcing through greenhouse gases or *vice versa* by albedo feedback.
- iv. Minimum SW monsoon precipitation was observed at LGM based on the oxygen isotope analysis as well as calcareous productivity.
- v. At T IA, an increase in SW monsoon precipitation is observed as evident from the negative $\delta^{18}\text{O}$ values due to influx of Bay of Bengal water, which is of lower salinity due to glacier melting and higher river runoff.
- vi. During the Holocene, SW monsoon intensified uniformly upto the core top as revealed by oxygen isotopes and calcareous productivity.
- vii. Calcareous productivity indicates a decreasing IEW and hence decreasing Indian and east African rainfalls upto LGM with a minimum value at LGM with the maximum El Nino frequency during the last glacial period. Thereafter the IEW strengthened upto 16.5 ka BP after which it fell back sharply to LGM values for a millennium, (~15.5 ka BP) indicating a reduction in rainfall. Thereafter IEW exhibit a sharp increase at ~14.5 ka BP that coincides with the Termination IA implying strengthened Southwest monsoon and East African rains.
- viii. Since ~14.5 ka BP to the core top (~2.2 ka BP) including the Holocene, calcareous productivity exhibits a uniformly increasing trend implying a uniformly strengthening IEW and Southern oscillation index and hence

strengthening SW monsoon and east African rains along with a declining El Nino frequency.

- ix. Based on the comparative study from the other two cores from the eastern Arabian Sea, it could be inferred the IEW and SW monsoon winds strengthened and weakened in unison pointing towards a common forcing factor, most probably insolation, at least during the last 35 ka.
- x. Spectral analyses of various proxies indicate that SW monsoon is dominated by the quasi-period of the precessional cycle, which indicates that it is governed by the solar forcing on the Milankovitch timescale. Common periodicity between the equatorial and north Atlantic records points towards a possible common mechanism linking them.
- xi. C_{org} and $\delta^{15}N$ are not useful as productivity indicators in this region because of the very little amount of sedimentary organic matter.
- xii. $\delta^{13}C$ of the foraminifera also is not useful as a productivity indicator in this region as the signal is mixed, caused by two processes viz. upwelling and productivity.